Supporting information

Multiplexed Self-Powered Biosensor for Ultrasensitive On-Site Detection of Trace Cisplatin via Catalytic Repurposing

Linlin Wang,[*a] Mengjie Jing,[a] Dongyan Lu,[b] Yuxin Wang,[b] Mingming Luo,[a] Guang Chen[*a], Qianhao Min[*b]

[a] Shaanxi Key Laboratory of Chemical Additives for Industry, Key Laboratory of Chemical Additives for China National Light Industry, College of Chemistry and Chemical Engineering, Shaanxi University of Science and Technology, Xi'an 710021, China

[b] State Key Laboratory of Analytical Chemistry for Life Science, School of Chemistry, Nanjing University, Nanjing, China.

E-mail: wanglinlin@sust.edu.cn; chenandguang@163.com; minqianhao@nju.edu.cn

Experimental Section

Materials and chemicals:

All chemicals were of analytical grade and used as purchased without further purification. High-purity single-walled carbon nanotubes (SWCNTs) were obtained from Suzhou Tanfeng Technology Reagent Co., Ltd. Concentrated sulfuric acid and hydrochloric acid were procured from Shanghai Macklin Biochemical Technology Co., Ltd., while nitric acid was supplied by Shanghai Aladdin Biochemical Technology Co., Ltd. Potassium ferricyanide was sourced from Shanghai Adamas-beta® Reagent Co., Ltd. Ferric chloride, N-Hydroxysuccinimide (NHS), and 1 – Ethyl – 3 - (3 - dimethylaminopropyl) carbodiimide Hydrochloride (EDC) were acquired from Shanghai Titan Scientific Co., Ltd. Potassium chloride and L-cysteine were procured from Shanghai Macklin Biochemical Technology Co., Ltd. and Sa'en Chemical Technology (Shanghai) Co., Ltd.,respectively. Cisplatin (cis-Diamminedichloroplatinum) and ascorbic acid (AA) were purchased from Beyo Pharmaceutical Co., Ltd. and Tianli Chemical Reagent Co., Ltd., respectively. Carbon Paper electrodes and indium tin oxide (ITO) electrodes were obtained from Wuhan Gausser Union Technology Co., Ltd. A 0.01 mol/L phosphate buffer solution (PBS, pH = 7.4) prepared from Na_2HPO_4 and KH_2PO_4 served as the supporting electrolyte. All solutions were prepared using ultrapure water (≥ 18 MΩ cm) from a Millipore Milli-Q system.

Apparatus:

Fourier transform infrared (FTIR) spectrometer was performed using a Bruck INVENIO spectrometer (Germany). Contact angle measurements were carried out with a Data Physics OCA20 optical contact angle meter (Germany). X-ray powder diffraction (XRD) patterns were recorded on a Bruker D8 Advance diffractometer (40 kV,40 mA) using Cu Kα radiation (λ = 1.54056 Å) at room temperature. Transmission electron microscopy (TEM) images were acquired with a JEOL 2800 microscope (Japan), while scanning electron microscopy (SEM) were performed using a JSM-7800F instrument (JEOL, Japan). Electrochemical measurements, including cyclic voltammetry (CV), linear sweep

voltammetry (LSV), and electrochemical impedance spectroscopy (EIS) (frequency range: 0.1 Hz to 100 kHz), were conducted on a CHI660E electrochemical workstation (CH Instruments, Shanghai) using a three-electrode system consisting of a platinum wire counter electrode, an Ag/AgCl reference electrode, and a working electrode.

Fabrication of SCNTs:

Precisely 30 mg of high-purity single-walled carbon nanotubes was dispersed in 30 mL of a H_2SO_4/HNO_3 mixture (3:1, v/v). The dispersion was sonicated for 10 h in an ice-water bath to achieve uniform dispersion, followed by dilution and overnight standing to ensure complete carboxylation. The product was then separated by centrifugation, vacuum-filtered through a 0.2 μm microporous membrane, and repeatedly washed with deionized water until a neutral pH was achieved. The collected solid material was carefully peeled from the membrane and dried at 50 °C for 24 h to obtain SCNTs powder. For subsequent application, the powder was dispersed in 0.1 M phosphate-buffered saline (PBS, pH 7.4) to prepare a 1 mg/mL suspension.

Fabrication of L-Cys/SCNTs anode:

First, 80 μL of the SCNTs dispersion was precisely drop-cast onto a pre-treated carbon paper electrode (1 cm × 1 cm) and vacuum-dried at 39 °C for 4 h to cure the film. To further immobilize the capture reagent for cisplatin detection, the SCNTs electrode was immersed in an EDC/NHS solution (1 mg/mL) for 30 min to activate the carboxyl groups on the SCNTs surface, followed by overnight immersion at 4 °C in an L-cysteine (L-Cys) solution to facilitate immobilization of L-Cys via amide linkage. Finally, the sensing anode of L-Cys/SCNTs was successfully fabricated.

Preparation of the PB cathode:

The PB cathode was fabricated via electrodeposition in a three-electrode system, in which the Ag/AgCl electrode, Pt plate, and indium tin oxide (ITO) served as the reference electrode, counter electrode, and working electrode, respectively. Specifically, the cleaned ITO electrode was immersed into an electrolyte solution containing 2.5 mM $K_3[Fe(CN)_6]$, 0.1 mM KCl, 2.5 mM $FeCl_3$ and 0.1 M HCl. The PB cathode was fabricated by applying a constant voltage of 0.4 V for 500 s.

Operation process of the MSPB:

The MSPB was assembled by connecting the L-Cys/SCNTs anode and the PB cathode. The MSPB was operated according to the following procedure for the detection of trace cisplatin: First, the device was immersed in samples containing cisplatin for 3 minutes. Subsequently, ascorbic acid (10 mM) was added to the anode chamber, and both the electrical signal and the colorimetric signal were recorded at predetermined time intervals.

Signal recording procedure for MSPB:

The MSPB was operated under a 0 V applied bias condition. The electrical signal was recorded by measuring the current-time characteristics of the MSPB. Meanwhile, the colorimetric signal of the MSPB was recorded by capturing the images of the PB cathode at regular intervals of 1 minute using a smartphone. The acquired images were then processed by RGB decomposition, and the intensity of the blue (B) channel was extracted for analysis.

Evaluation of the electrochemical performance of the MSPB:

First, the operation stability of the MSPB was evaluated by monitoring its long-term open-circuit voltage output. Subsequently, the energy conversion efficiency of the MSPB was assessed by recording its power output. Specifically, the power output of the MSPB was calculated according to the following equation:

$$\boldsymbol{P = E_{cell} \times j}$$

where the E_{cell} and j represent the operating voltage (V), and the corresponding current response ($\mu A \cdot cm^{-2}$) of the MSPB, respectively.

Supporting Figures

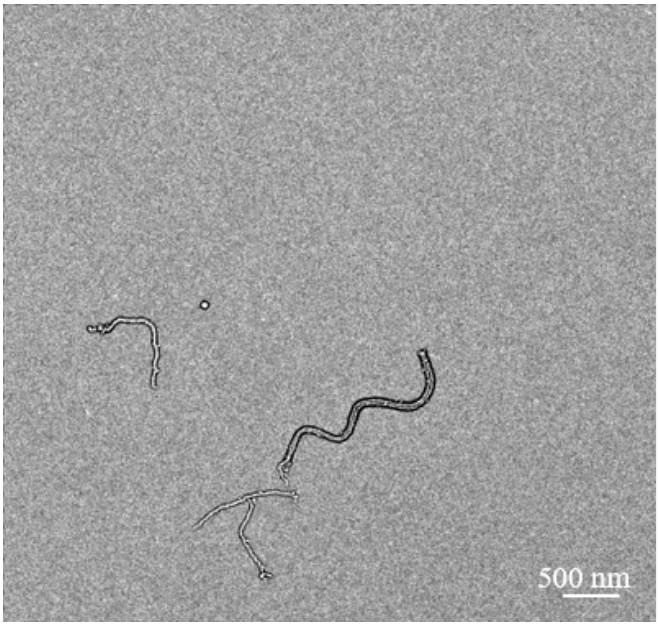

Fig. S1 The TEM images of SCNTs.

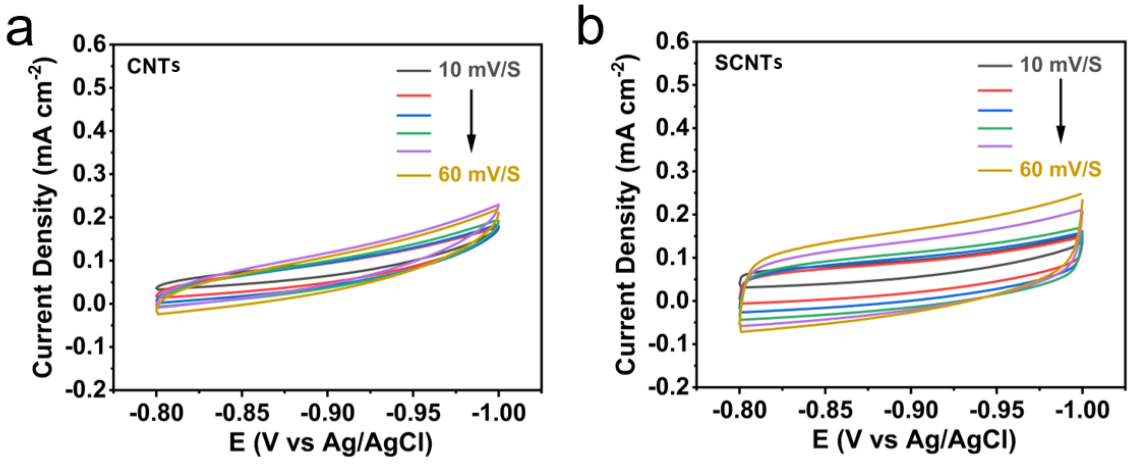

Fig. S2 CV curves of (a) CNTs electrode and (b) SCNTs electrode at different scan rates (from 10 mV s^{-1} to 60 mV s^{-1}).

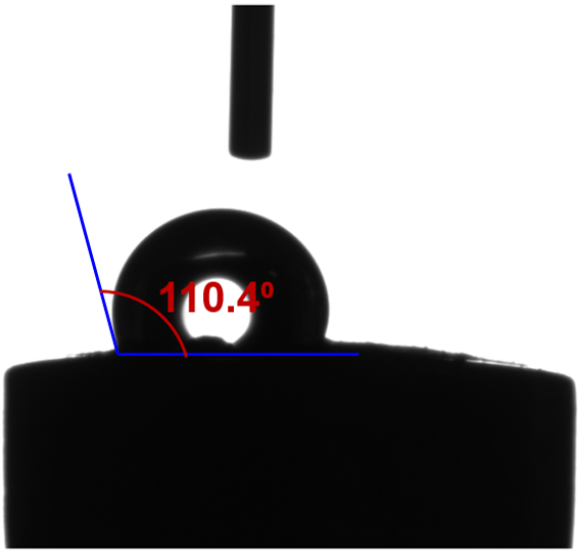

Fig. S3 Contact angle of the CNTs electrode.

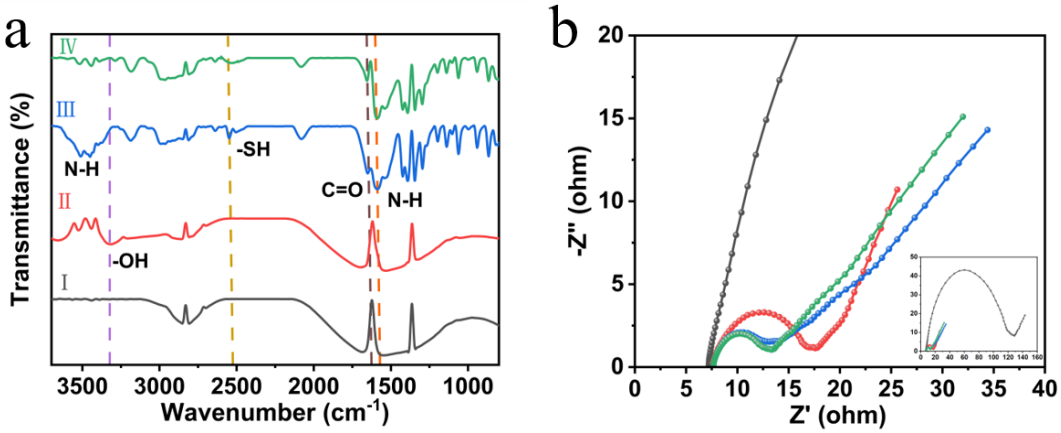

Fig. S4 (a) FTIR of (I) CNTs, (II) SCNTs, (III) L-Cys/SCNTs. (b) Nyquist plots measured at the open-circuit voltage of bare carbon paper electrode (black), SCNTs (red), L-Cys/SCNTs (bule), and cDDP/ L-Cys/SCNTs (green).

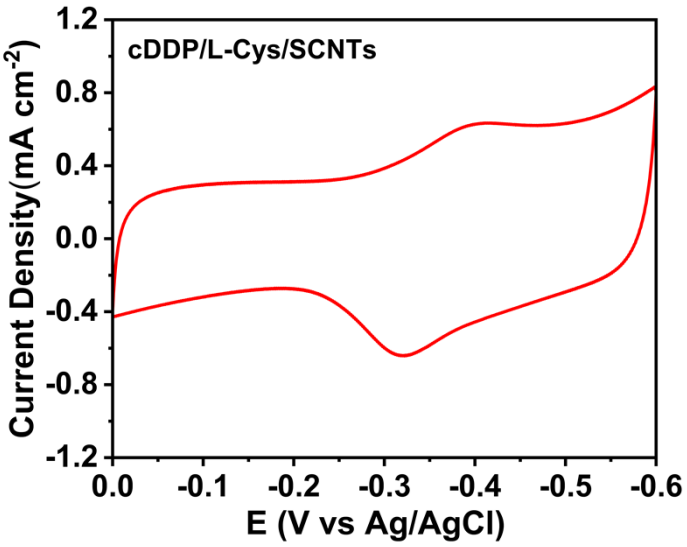

Fig. S5 Cyclic voltammetry curves of the cDDP/L-Cys/SCNTs anode in PBS.

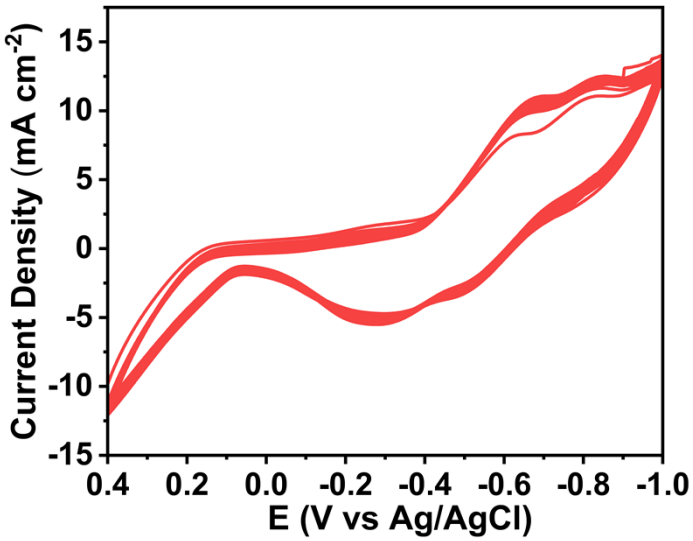

Fig. S6 Cyclic voltammetry curves of the cDDP/L-Cys/SCNTs anode in AA solution.

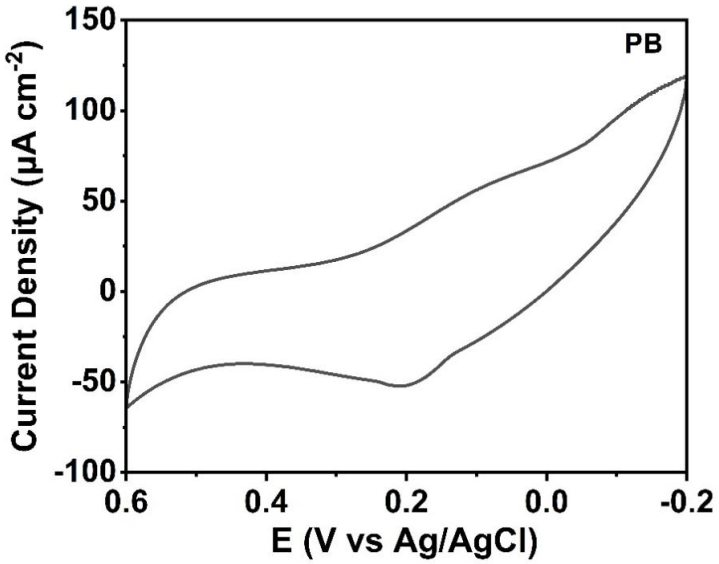

Fig. S7 Cyclic voltammetry (CV) characterization of Prussian blue (PB) cathode.

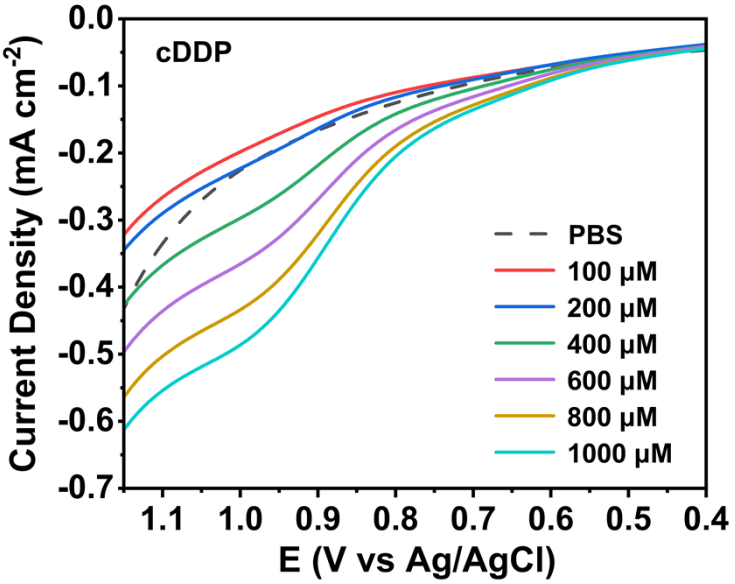

Fig. S8 LSV curves of the direct electro-oxidation of cDDP at varying concentrations.

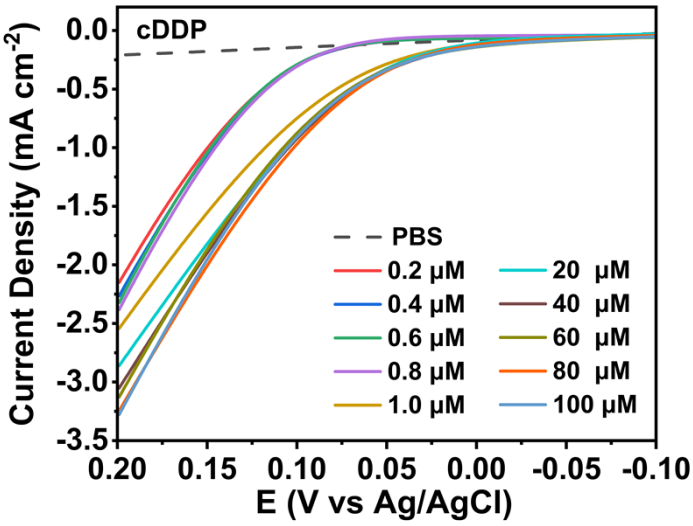

Fig. S9 LSV curves of the L-Cys/SCNTs sensing anode incubated with varying cDDP concentrations.

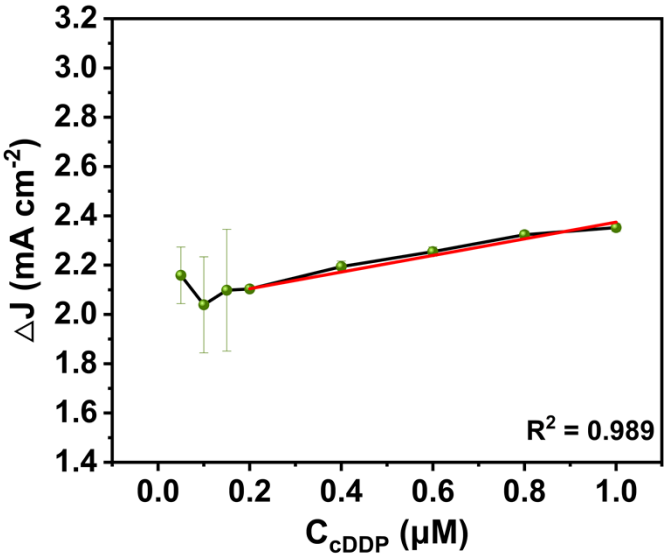

Fig. S10 Standard calibration curves of current response (ΔJ) versus cDDP concentration at the L-Cys/SCNTs anode under low C_{cDDP} concentrations.

.

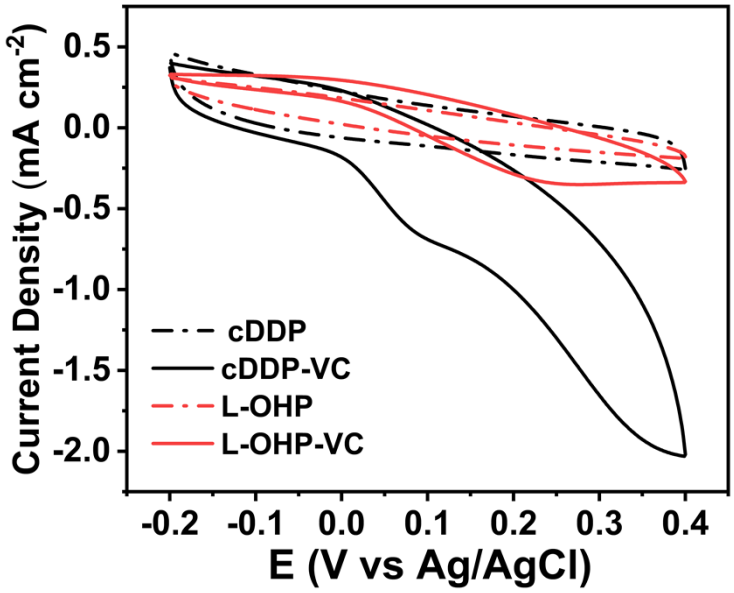

Fig. S11 CV curves of the cDDP/L-Cys/SCNTs anode (black) and the OHP/L-Cys/SCNTs anode (red) in response to AA.

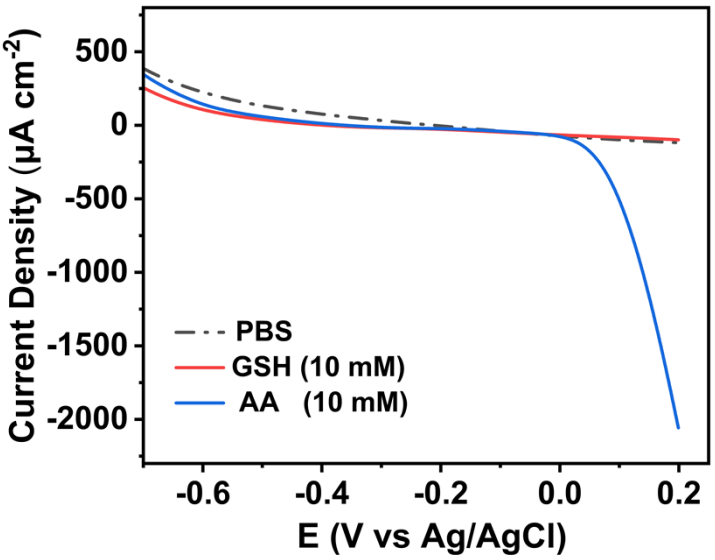

Fig. S12 LSV curves of the cDDP/L-Cys/SCNTs sensing anode in electrolyte containing 10 mM AA (blue curve) and 10 mM GSH (red curve).

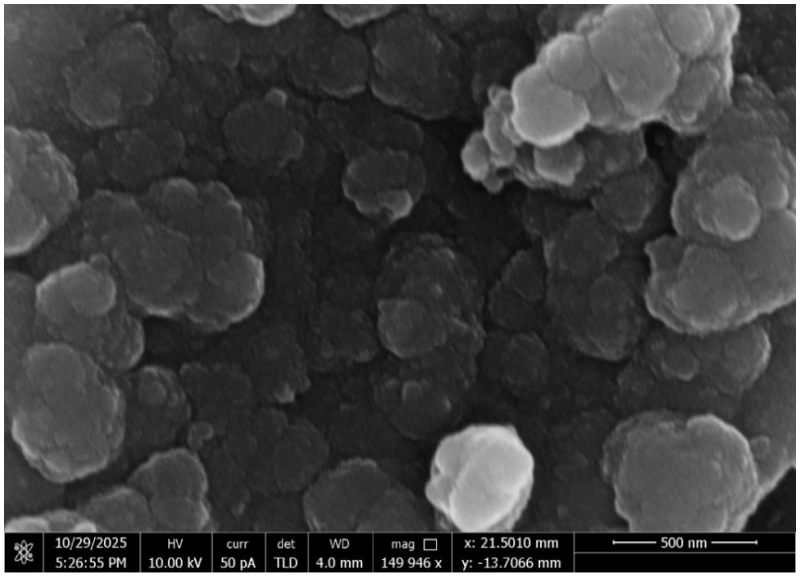

Fig. S13 SEM image of the PB cathode.

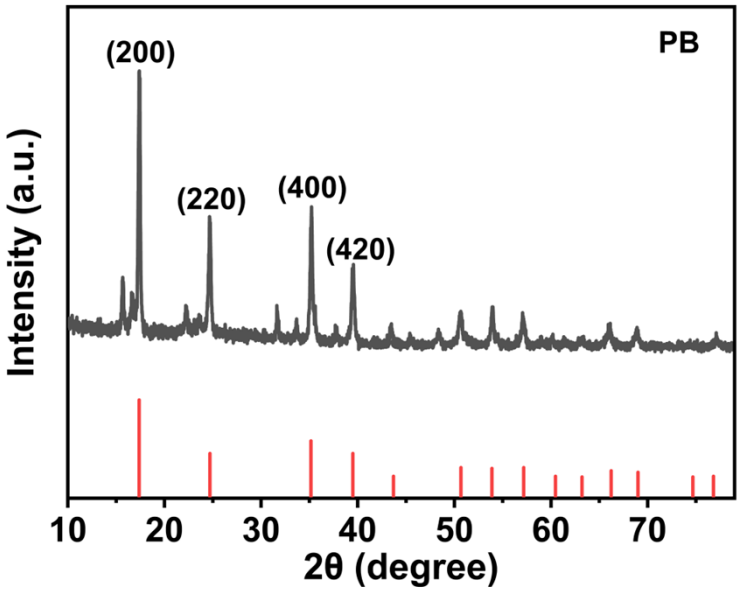

Fig. S14 X-ray diffraction (XRD) pattern of PB.

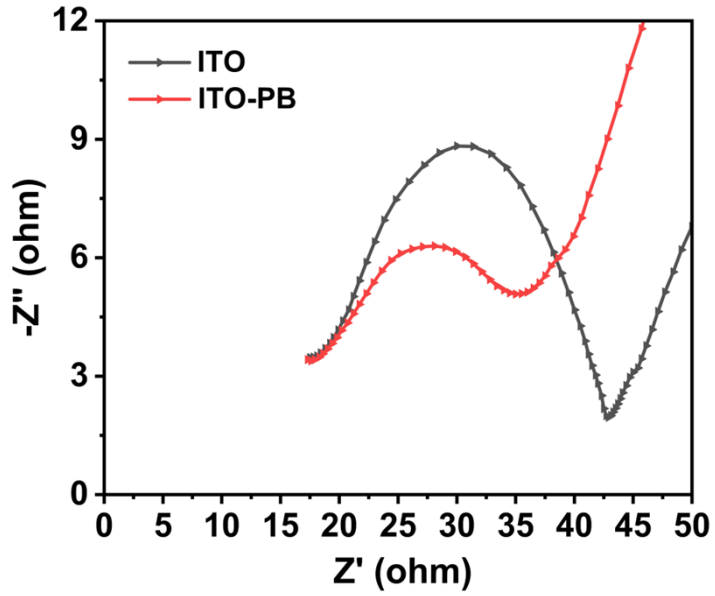

Fig. S15 EIS rspectra of the bare ITO electrode (black) and PB/ITO electrode (red).

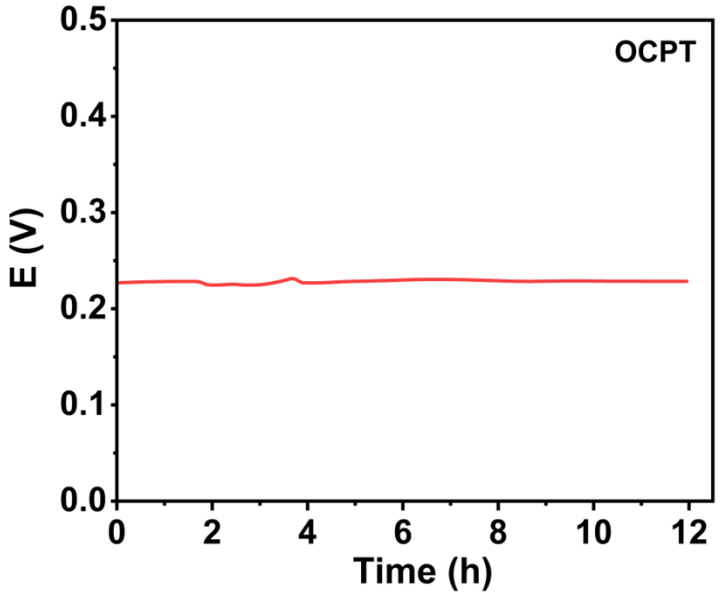

Fig. S16 The open-circuit voltage versus time curve of the MSPB.

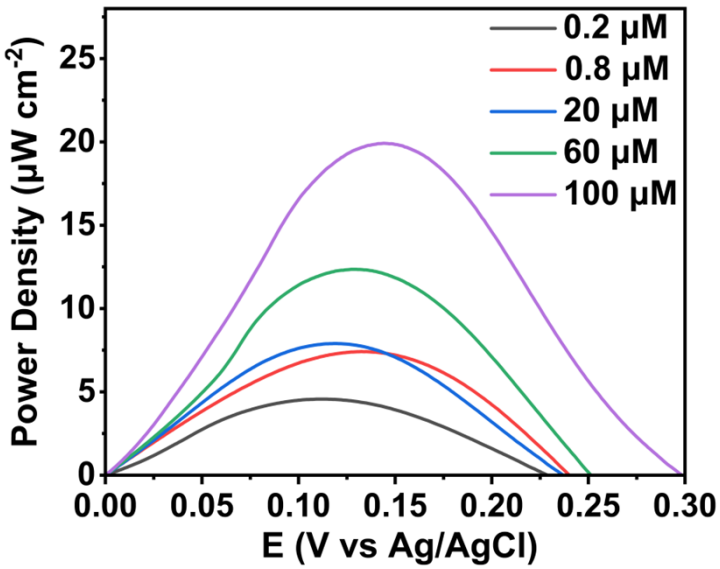

Fig. S17 Power density curves of the MSPB following a 3-min immersion in samples containing varying concentrations of cisplatin; scan rate: 5 mV s^{-1}.

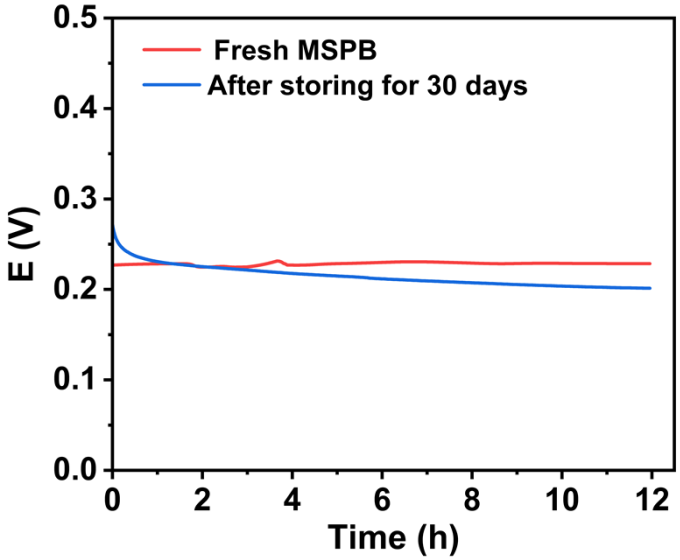

Fig. S18 The open-circuit voltage versus time curve of the MSPB.

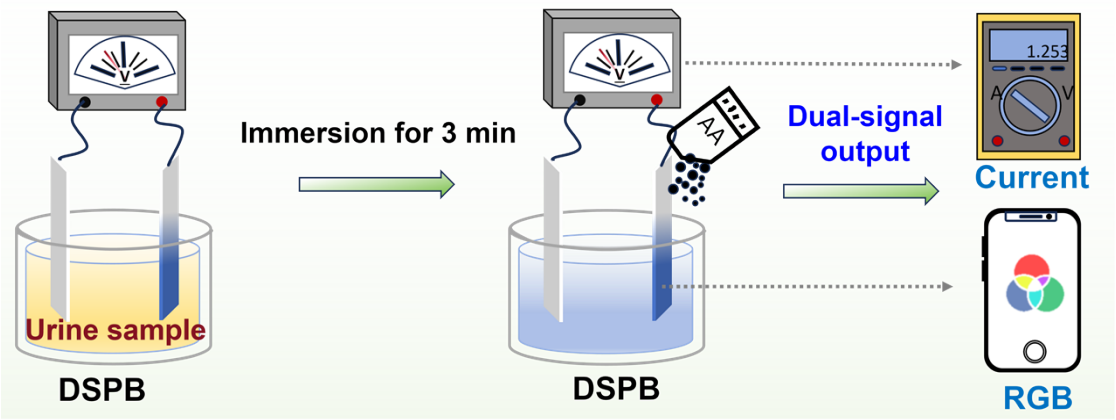

Fig. S19 Working principle of the MSPB integrating L-Cys/SCNTs anode and PB cathode.

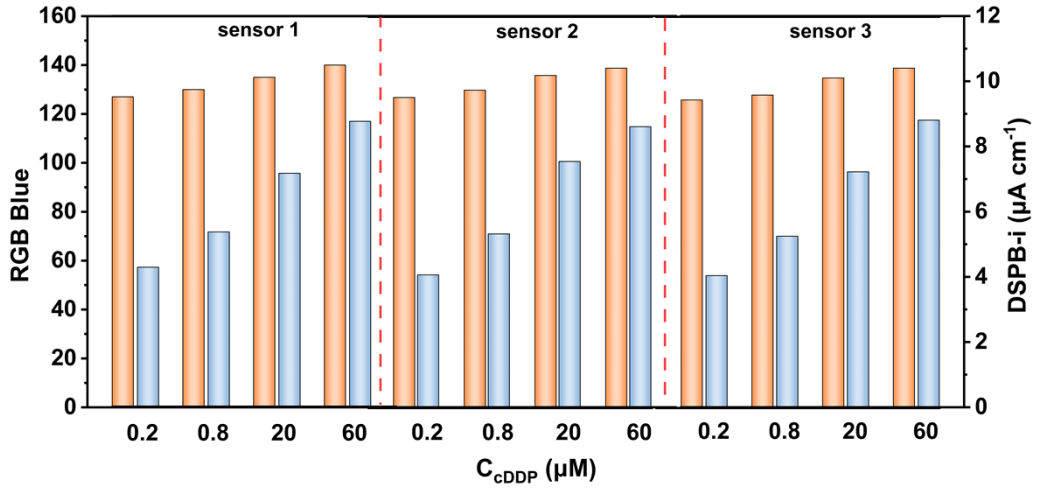

Fig. S20 Electrical (blue) and colorimetric (orange) readouts of the MSPB in urine spiked with cDDP (0.2–60 μM).

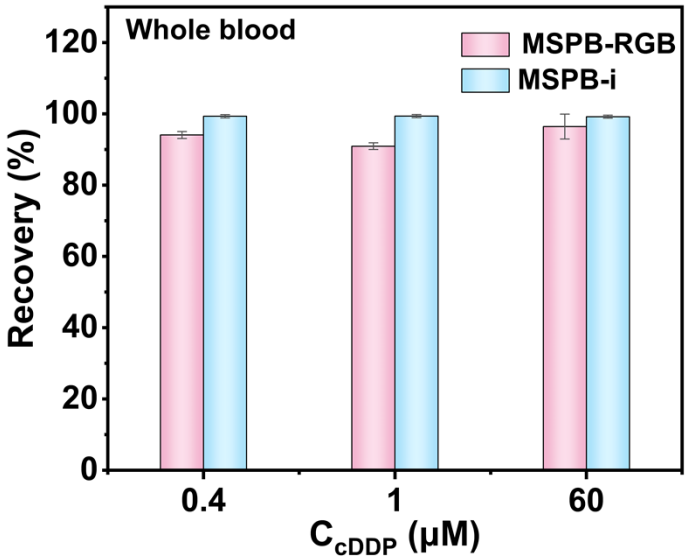

Fig. S21 Electrochemical and colorimetric recovery rates of cisplatin at various concentrations in whole blood.

POC Platform / Sensor Type	Detection Principle	Target Analyte	Linear Range	LOD	Detection Time	Ref.
Wearable Microneedle Sensor	Aptamer + Electrochemistry	Glucose / Lactate	Not specified	High specificity	Real-time / Continuous	Adv. Mater. 2024;36:2313743.
Plug-In Paper-Based Biosensor	Internal Standard Peptide Immunochromatography	Procalcitonin (PCT)	0.003 – 100 (ng/mL)	0.002 ng/mL	< 25 min	Talanta 2026, 299:129112.
MIP-based Electrochemical Sensor	Molecularly Imprinted Polymer	CEA	6.25 -100 (ng/mL)	2.0 ng/mL	Not specified	Microchem. J. 2025;218:115548.
Wearable MIP Sensor	MIP + Deep Learning	MMP-8	Not specified	High specificity	Real-time / Continuous	Adv. Sci. 2025;:2509658.
This work	**0.2 ~ 100 0.2 ~ 100**	**Cisplatin**	**0.2 – 100 (μM)**	**86 nM**	**< 3 min**	**/**

Fig. S22 Performance comparison of current POC devices.

Method	Linear rang (μM)	LOD (μM)	Conditions	Real sample	Pretreatment	Recovery (%)	Ref.
Fluorescence	0 ~240	0.13	HEPES (pH = 7.4)	Urine	Deproteinization	89.8 ~ 91.6	J. Am. Chem. Soc. 2024;146(49).
Fluorescence	0 ~ 100	0.08	HEPES (pH = 7.4)	/	/	/	Angew. Chem. Int. Ed. 2021;60(17).
DPASV	0.2 ~110	0.09	PBS, KCl (pH = 7.0	Urine	Deproteinization	98 ~ 104	Sens. Actuators B: Chem. 2019;299.
DPV	6.0 ~ 180	4.4	PBS (pH = 5.5)	Serum	Deproteinization	89 ~102	Talanta 2024;267.
SWV	50 ~ 140	8.8	PBS (pH = 6.5)	/	/	/	Biosens. Bioelectron. 2014;58.
ACV	0.2 ~ 2	0.2	HEPES, $NaClO_4$ (pH = 5.0)	50% Urine	Dilution	/	Anal. Chem. 2017;89(18).
DPV	1.30 ~ 26.0	0.113	KCl (pH=7.4)	5% Serum	Dilution	93.2~104.9	Int. J. Electrochem. Sci. 2014;9(1537-1546).
CV	1.0 ~ 100	0.5	KCl (pH=7.4)	Urine	Filter	70~90	Electroanalysis. 2025; 37.
DPV	14.5 ~ 100	14.0	NaCl (pH=7.4)	Serum	Centrifuge	/	Electrochim. Acta. 2015;158(271-276).
SWV	1.0 ~ 2000	1.0	PBS (pH = 7.4)	Serum	/	90~105	Microchem. J.2026; 221(116962).
DSPB-RGB DSPB-i	**0.2 ~ 100 0.2 ~ 100**	**0.097 0.086**	**PBS (pH = 7.4)**	**Urine**	**Without sample preprocessing**	**98.7 ~ 99.2 96.1 ~ 98**	**This work**

Fig. S23 Analytical performance comparison of cisplatin sensors.

Table S1 Statistical comparison of recovery rates and standard deviations between the MSPB and ICP-MS methods.

cDDP in Urine (μM)	ICP-MS Recovery (%)	Anodic current Recovery (%)	SD	MSPB-i Recovery (%)	SD	MSPB-RGB Recovery (%)	SD
0.8	97.5	99.59	0.62	96.13	1.07	98.78	0.88
20	92.5	98.41	1.15	90.91	2.52	98.09	0.42
60	110.67	97.39	1.49	98.01	1.14	99.26	0.41